

## Extension of the Norsand Model to Capture the Hydromechanical Behavior of Unsaturated Gold Mine Tailings

Mina Mofrad<sup>1</sup>, Mehdi Pouragha<sup>\*,1</sup>, and Paul Simms<sup>1</sup>

<sup>1</sup>*Department of Civil and Environmental Engineering, Carleton University, Ottawa, Canada*

*\*Corresponding author's email:* mehdi.pouragha@carleton.ca

**Abstract:** Hard rock tailings, composed primarily of low-plasticity sands and silts with broad particle size distributions, exhibit a wide water retention curve and significant hydraulic hysteresis during drying and wetting cycles. In certain climates and deposition scenarios, tailings undergo complex hydro-mechanical stress paths, including repeated desiccation and rehydration cycles, which significantly affect their shear behavior. Existing constitutive models for unsaturated soils, such as the Barcelona Basic Model and Glasgow Coupled Model (GCM), are largely based on Cam-Clay theory and are primarily suited for clayey materials. However, the frictional nature of hard rock tailings demands models that account for plastic dilatancy and unique volumetric responses. This study extends the Norsand dilatancy-based constitutive model by incorporating key elements of the GCM framework, introducing two additional hydraulic yield surfaces, and establishing coupling between hydraulic and mechanical processes. The enhanced model is calibrated and validated using triaxial and simple shear tests conducted on unsaturated gold mine tailings. Results demonstrate the model's ability to accurately capture essential features of tailings' shear behavior, providing a robust tool for analyzing their hydro-mechanical response under varying stress paths and unsaturated conditions.

### Introduction

Hard rock tailings are the residual by-products of mineral extraction from rock deposits, typically deposited as slurries due to the water used in mineral processing. In certain climates and under specific deposition practices, such as filtered or thickened tailings, these materials can undergo complex hydro-mechanical loading histories characterized by repeated cycles of desiccation and saturation. In multilayer deposition, such stress histories involve self-weight consolidation, followed by desiccation, and subsequently, rewetting as new layers are added [1, 2]. These cycles of drying and wetting can induce significant changes in the tailings' structure, with past desiccation strongly influencing their strength behavior, even after full re-saturation [3, 4].

During desiccation, tailings enter an unsaturated state and undergo irreversible structural changes, leading to distinct hydro-mechanical behavior upon rewetting. This behavior transcends traditional soil mechanics, which primarily address dry or fully saturated soils. Contemporary unsaturated soil mechanics incorporates new concepts, such as matric suction, coupled hydraulic and mechanical behavior, and hysteretic effects associated with drying and wetting

cycles [5, 6]. Accurate prediction of such behavior requires constitutive models that account for these complexities.

The concept of effective stress has been extended to unsaturated soils by incorporating additional variables, such as matric suction [7]. However, unlike saturated soils, unsaturated soil behavior cannot be fully represented by a single stress state variable [8]. This limitation has led to the development of constitutive models incorporating additional state parameters and coupling terms to address unsaturated soil behaviors, forming a distinct branch of soil mechanics.

Early models, such as the Barcelona Basic Model (BBM) [9] and the Glasgow Coupled Model (GCM) [10], extended the Modified Cam Clay Model (MCC) [11] to unsaturated soils. However, these models focus primarily on clayey materials with high suction sensitivity and narrow soil-water characteristic curves (SWCCs). In contrast, hard rock tailings, composed of silts and sands with wide particle size distributions, exhibit broader SWCCs and pronounced hydraulic hysteresis during drying and wetting cycles. Their frictional and cohesionless nature necessitates constitutive models that go beyond classical Cam-Clay theory to accurately capture dilatancy and volumetric responses.

This study extends the hydromechanical coupling framework of GCM to a dilatancy-based constitutive model, Norsand [12], to better capture the behavior of granular materials under partially saturated conditions. Recent modifications [13] are integrated to improve the modeling of hydraulic hysteresis. The extended model is applied to unsaturated gold mine tailings, and its predictions are compared with GCM. The results demonstrate the model's capability to capture key trends in tailings behavior under complex hydromechanical loading conditions.

## Constitutive Model Formulation

This section provides a concise overview of the key aspects of the Norsand model. The following formulations define the hydrostatic and deviatoric components of the stress tensors along with their corresponding conjugate strain components:

$$\begin{aligned} p &= \frac{\sigma_{ii}}{3}, & q &= \sqrt{\frac{3}{2}s_{ij}s_{ij}}, & s_{ij} &= \sigma_{ij} - p\delta_{ij} \\ \varepsilon_v &= \varepsilon_{ii}, & \varepsilon_s &= \sqrt{\frac{2}{3}e_{ij}e_{ij}}, & e_{ij} &= \varepsilon_{ij} - \frac{1}{3}\varepsilon_v\delta_{ij} \end{aligned} \quad (1)$$

where  $\delta$  is the Kronecker delta, and repeated indices denote summation. The over dot  $\dot{X}$  represents incremental rate.

### Original Norsand Model

The Norsand model [12] is a generalized Cambridge-type constitutive model developed based on the fundamental assumptions of critical state theory. Initially, it was primarily used to model the mechanical behavior of sands. However, it has since been applied to soils with particle sizes ranging from silt to sand, aiming to capture their unique characteristics. The model adopts the

effective stress concept introduced by [14] as the stress state variable, defined as:

$$\sigma'_{ij} = \sigma_{ij} - u_w \delta_{ij} \quad (2)$$

where  $\sigma_{ij}$  is the total stress tensor and  $u_w$  is the pore water pressure.

The model employs nonlinear isotropic elasticity, with the bulk modulus  $K$  and shear modulus  $G$  defined as functions of the current mean effective stress  $p'$ :

$$\begin{aligned} \dot{\sigma}'_{ij} &= C_{ijkl} \dot{\varepsilon}_{kl} \\ C_{ijkl} &= (K - \frac{2}{3}G)\delta_{ij}\delta_{kl} + 2G \left[ \frac{1}{2}(\delta_{ik}\delta_{jl} + \delta_{il}\delta_{jk}) \right], \quad K = \frac{2(1+\nu)}{3(1-2\nu)}G, \quad G = I_r p' \end{aligned} \quad (3)$$

where  $\nu$  is Poisson's ratio and  $I_r$  is a material constant.

The Norsand model introduces a state parameter  $\psi$ , which controls dilatancy and is defined as the difference between the current void ratio ( $e$ ) and the critical void ratio ( $e_c$ ) at the same mean effective stress ( $p'$ ):

$$\psi = e - e_c, \quad e_c = \Gamma - \lambda \ln p' \quad (4)$$

where  $\Gamma$  and  $\lambda$  are material parameters describing the critical state line.

The model features a yield surface with a bullet-like shape, similar to the Cam Clay model, but cropped by a lower cap to better capture hysteresis during cyclic loading:

$$F = \frac{q}{p'} + M_i \left( \ln \left( \frac{p'}{p'_i} \right) - 1 \right) = 0 \quad \text{for} \quad \left( \frac{p'_i}{p'} \right) < \exp \left( -\frac{\chi_i \psi_i}{M_{i,tc}} \right) \quad (5)$$

The variables  $M_i$ ,  $\psi_i$ , and  $\chi_i$  depend on material constants and are defined as follows:

$$M_i = M \left( 1 - \frac{N \chi_i |\psi_i|}{M_{tc}} \right), \quad \chi_i = \frac{\chi_{tc}}{1 - \frac{\chi_{tc} \lambda}{M_{tc}}}, \quad \psi_i = \psi - \lambda \ln \left( \frac{p'_i}{p'} \right) \quad (6)$$

Here,  $N$  is a material constant, and  $M$  is the critical state slope in  $q-p'$  space, which depends on the Lode angle  $\theta$ :

$$M = M_{tc} - \frac{M_{tc}^2}{3 + M_{tc}} \cos \left( \frac{3}{2}\theta + \frac{\pi}{4} \right) \quad (7)$$

where  $M_{tc}$  is the slope of the critical state line along the triaxial compression path, and  $\chi_{tc}$  is a material parameter. The parameter  $M_{i,tc}$  refers to  $M_i$  for the triaxial compression condition:

$$M_{i,tc} = M_{tc} - N \chi_i |\psi_i|. \quad (8)$$

The yield surface is illustrated in Figure 1 for initially loose and dense samples. The size of the yield surface evolves with the image hardening parameter,  $p'_i$ , which is related to the change in plastic deviatoric strain increments,  $\dot{\varepsilon}_q^p$ :

$$\dot{p}'_i = p'_i H \frac{M_i}{M_{i,tc}} \left( \frac{p'}{p'_i} \right)^2 \left[ \exp \left( -\frac{\chi_i \psi_i}{M_{i,tc}} \right) - \frac{p'_i}{p'} \right] \dot{\varepsilon}_q^p \quad (9)$$

with  $H$  being plastic hardening modulus for loading. Different relationships for  $H$  are proposed as a function of  $\psi$  or  $\psi_0$  [15, 16].

Moreover, the Norsand model employs an associated flow rule.

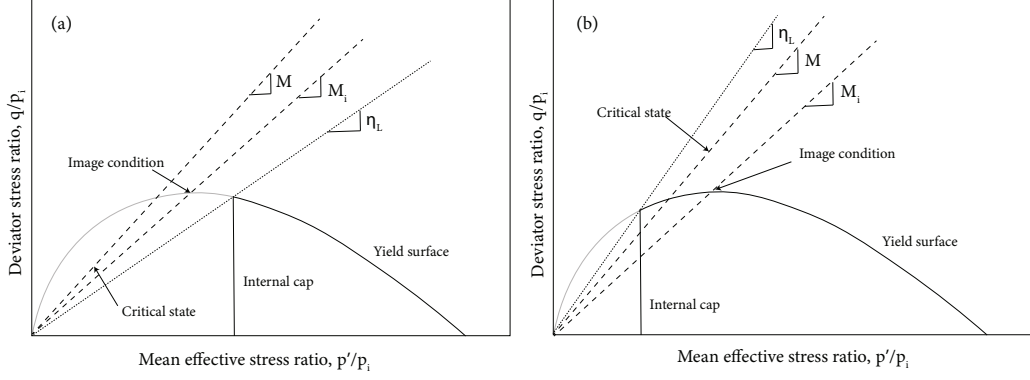


Figure 1: Yield surface of the Norsand model in stress ratio space, a) loose soil b) dense soils.

### Unsaturated Norsand Model

The original Norsand model (Jefferies, 1993) is developed for dry and saturated materials. In this study, we extend the model to account for unsaturated conditions by incorporating the framework presented in [13], which itself is based on the GCM framework. This extension involves three main steps: (1) selecting appropriate state variables for unsaturated materials, (2) introducing new constitutive relations to describe the evolution of the added state variables, specifically a suction-saturation relation, and (3) incorporating coupling terms into the evolution laws, such as those governing hardening.

Following the thermodynamic framework outlined by [17], we adopt Bishop's effective stress,  $\sigma^*$ , and modified matric suction,  $s^*$ , as the primary stress state variables. The total strain,  $\varepsilon$ , and the saturation ratio,  $S_r$ , serve as their energy conjugates, respectively:

$$\sigma_{ij}^* = \sigma_{ij} - (S_r u_w + (1 - S_r) u_a) \delta_{ij}, \quad s^* = n (u_a - u_w) \quad (10)$$

Here,  $\sigma$  represents the total stress tensor,  $u_a$  and  $u_w$  are the air and water pressures, and  $n$  is the porosity. By explicitly considering  $s^*$  and  $S_r$  as energy conjugates, the Extended Norsand model is better equipped to capture the transition between saturated and unsaturated states, while also incorporating the influence of retention hysteresis more accurately.

In a manner similar to the GCM, the yield surface in the Extended Norsand model is extended into a third dimension corresponding to  $s^*$ . Two additional caps describing the hydraulic yield surfaces are introduced as follows:

$$F_{SI} = s^* - s_I^* = 0, \quad F_{SD} = s_D^* - s^* = 0 \quad (11)$$

where  $s_I^*$  and  $s_D^*$  are parameters whose evolution (hydraulic hardening) will be defined later.

The additional constitutive relation for the newly introduced hydraulic state variables is expressed through a suction-saturation curve (SWCC), which is modeled as a family of S-shaped curves. These curves follow the general form of the well-known Van Genuchten expression [18]. The hardening of the hydraulic yield surfaces is assumed to occur in such a way that the modified suction and saturation evolve according to the following equation:

$$S_r = \left(1 + (as^*)^b\right)^{-m} \quad (12)$$

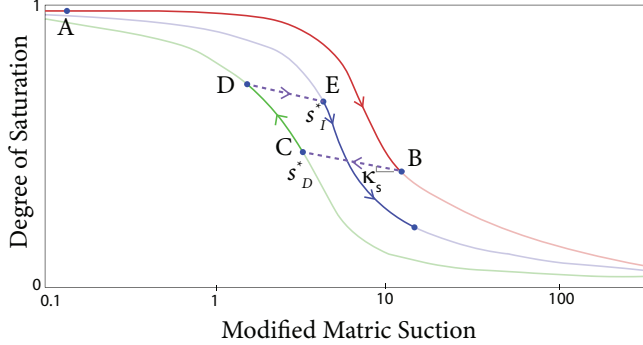


Figure 2: Example of scanning curves during drying and wetting paths.

Here,  $a$  and  $b$  are model constants, while  $m$  is a parameter determined based on the material's state at the onset of hydraulic yielding. After hydraulic yielding, the hydraulic state follows the curve described by Eq. 12, while during reversible hydraulic processes, the state rebounds along a semi-logarithmic line with a constant slope of  $\kappa_s$  until the next hydraulic surface is reached. Upon the first instance of yielding, the parameter  $m$  is updated such that the current material state corresponds to a curve within the family described by Eq. 12, and this value remains fixed during continuous yielding. A schematic of these scanning curves and log-linear hydraulic rebound curves is shown in Figure 2.

The hardening laws for the parameters describing the size of the yield surfaces are modified to include coupling terms, similar to the GCM. These laws are given by:

$$\dot{p}'_i = p'_i \left[ H \frac{M_i}{M_{i,tc}} \left( \frac{p^*}{p'i} \right)^2 \left( \exp \left( \frac{-\chi_i \psi_i}{M_{i,tc}} \right) - \frac{p'_i}{p^*} \right) \dot{\varepsilon}_q^p + k_1 \frac{\left( 1 + (as_x^*)^b \right)^{1+m}}{bm (as_x^*)^b} (-\dot{S}_r^p) \right] \quad (13)$$

$$\dot{s}_x^* = s_x^* \left[ \frac{k_2 H M_i}{M_{i,tc}} \left( \frac{p^*}{p'i} \right)^2 \left( \exp \left( -\frac{\chi_i \psi_i}{M_{i,tc}} \right) - \frac{p'_i}{p^*} \right) \dot{\varepsilon}_q^p + \frac{\left( 1 + (as_x^*)^b \right)^{1+m}}{bm (as_x^*)^b} (-\dot{S}_r^p) \right] \quad (14)$$

where  $k_1$  and  $k_2$  are model parameters. The evolution of the yield surface is governed by the hardening parameters,  $\dot{p}'_i$ ,  $\dot{s}_x^*$ , and  $\dot{s}_D^*$ , expressed in terms of plastic deviatoric strain increments,  $\dot{\varepsilon}_q^p$ , and the plastic increments of the degree of saturation,  $\dot{S}_r^p$ . As with the original Norsand model, the flow rule associated with the frictional and hydraulic yield surfaces remain associated.

## Results

The Extended Norsand model has been implemented using an explicit numerical integration method. The model was then calibrated and applied to reproduce the behavior of unsaturated tailings. The experimental dataset, extracted from [3] and [4], aims to investigate the effect

of hydraulic stress history on the mechanical behavior of unsaturated gold mine tailings. Soil specimens were initially prepared as a slurry with a 38% water content, and two layers of tailings, each with a thickness of 10 cm, were sequentially deposited in a cylindrical column with a diameter of 25 cm. The bottom layer underwent self-weight settling, followed by desiccation to three different gravimetric water contents:  $W_d = 23\%$ , 17%, and 12%. The specimens were then rewetted to a saturated condition once the second layer was placed. The soil samples collected from the bottom layer, which experienced drying to various water content levels, were saturated and their water content consistently ranged from 21% to 22%. The extracted samples were then placed in a simple shear apparatus and consolidated under a vertical effective stress of 50 kPa, followed by undrained shear loading.

The testing results during the desiccation/rewetting and shearing processes were used to calibrate the constitutive model. Specifically, the behavior during rewetting and at the initial stages of shearing were used to calibrate the elastic properties, while the results at the end of the shearing test were used to calculate parameters associated with characterizing the critical state. The 14 calibrated parameters are as follows:  $\nu = 0.2$ ,  $N = 0.1$ ,  $\Gamma = 0.95$ ,  $M_{tc} = 1.2$ ,  $x_{tc} = 4.7$ ,  $I_r = 55$ ,  $\lambda = 0.035$ ,  $k_1 = 0.6$ ,  $k_2 = 0.1$ ,  $a = 0.045$ ,  $b = 0.8$ ,  $m = 0.4$ ,  $\kappa_s = 0.001$ . A power-law relationship is adopted for  $H$  as a function of  $\psi_0$  as  $H = H_{ref}|\psi_0|^{-r}$  in which  $H_{ref} = 250$  and  $r = -1.4$ . Due to structural changes induced by hydraulic loading (desiccation and rewetting), the void ratio and corresponding state parameter ( $\psi$ ) evolve, influencing the mechanical response. To account for these changes,  $H$  was recalculated once after hydraulic loading, immediately prior to the mechanical consolidation phase, using the updated state parameter ( $\psi$ ). This discrete update ensures that  $H$  accurately reflects the altered state of the material after hydraulic processes, aligning the model predictions with experimental observations. By avoiding continuous recalculations, the approach balances computational efficiency with physical accuracy, capturing the significant effects of hydraulic history on shear hardening without overcomplicating the implementation.

Figures 3 and 4 illustrate the comparison between the predictions from the Extended Norsand model and the experimental results, represented by square symbols. To facilitate a better comparison, the results from the Modified Glasgow Coupled Model (MGCM), as developed by [13], are also included. Figure 3 depicts the variation in void ratio as a function of suction stress and net normal stress for two different samples. In contrast, Figure 4 displays the shear stress versus shear strain relationship, alongside the effective stress path. To enhance visualization, the evolution of the yield surfaces for the Extended Norsand model in both the  $p^* - s^*$  and  $p^* - q$  spaces is shown in Figure 5 for a sample that underwent desiccation to  $W_d = 12\%$ .

## Discussion

The performance of the Extended Norsand constitutive model was evaluated against the MGCM in predicting the shear response of desiccated and rewetted gold tailings. Both models demonstrated realistic trends in capturing void ratio changes during desiccation, rewetting, and consolidation. The realistic representation of these changes, as shown in Figure 4, is attributed to the robust hydro-mechanical coupling and the effective relationship between suction and saturation ratio incorporated in the Extended Norsand model.

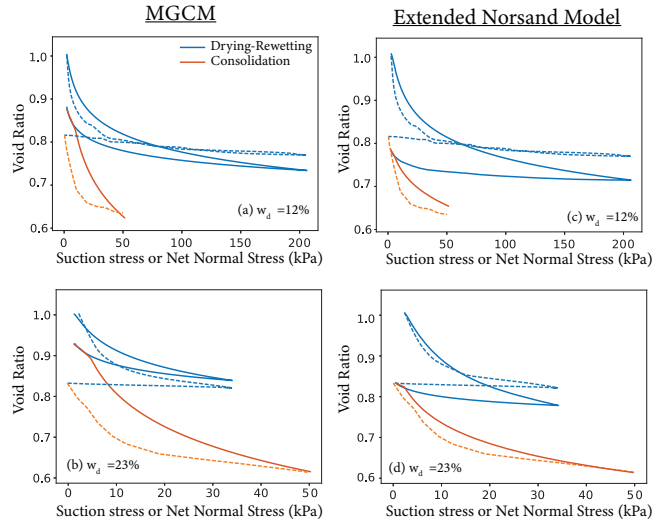


Figure 3: Comparison between experimental results (dashed lines) and model predictions (solid lines) for volume change. The samples are desiccated to  $W_d = 12\%$  (a, c) or  $W_d = 23\%$  (b, d), subsequently rewetted to a fully saturated state, and then consolidated to 50 kPa.

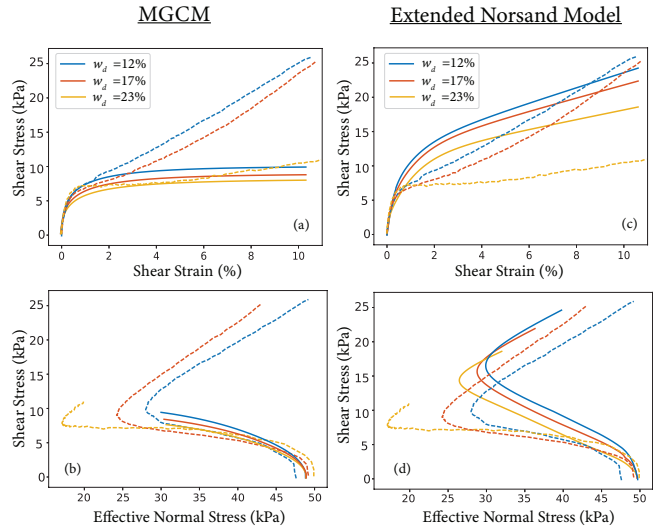


Figure 4: Comparison between the experimental results (dashed lines) and the model predictions (solid lines); (a, c) shear stress vs strain, and (b, d) simple shear effective stress path.

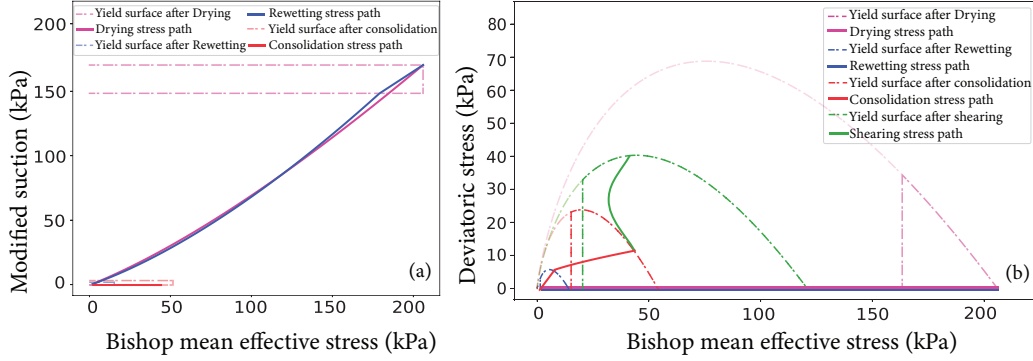


Figure 5: The evolution of the yield surfaces for the Extended Norsand model for the sample with  $W_d = 12\%$ . (a) Hydromechanical yield surface in the  $p^* - s^*$  space, and (b) mechanical yield surface in the  $p^* - q$  space.

During the initial drying stage, illustrated in Figure 5, the soil lies on the SI hydraulic yield surface and undergoes yielding as water content decreases, resulting in an expansion of the elastic zone in both hydraulic and mechanical domains. Upon rewetting, the soil exhibits elastic behavior until it reaches the SD yield surface. Beyond this point, the soil begins to yield, and the coupling between hydraulic and mechanical behaviors causes the mechanical yield surface to contract. This contraction during rewetting leads to yielding during consolidation, effectively reproducing the observed experimental trends in void ratio changes.

In terms of shearing response, the Extended Norsand model offers more realistic predictions compared to MGCM. This superiority arises from its non-associated plastic flow rule and hardening mechanism with plastic shear strain (Eq. 19), which enables an asymptotic approach to the critical state line. Unlike models such as GCM, the Extended Norsand model allows the critical state values for stress and void ratio to evolve independently. Consequently, the state of the material can approach the critical state slope in the  $q - p$  space without the void ratio necessarily reaching its critical state value. This allows stresses to asymptotically evolve toward the critical state line in the  $q - p$  space, even when a true critical state is not realized.

The model successfully captures the general trend of increasing shear strength with intensified desiccation. However, its accuracy diminishes for samples with lower levels of desiccation ( $w_d = 23\%$ ), particularly in predicting the effective normal stress at failure (end of solid lines). Moreover, as shown in Figure 4, the Extended Norsand model effectively captures the increase in shear hardening behavior with greater levels of desiccation.

Finally, the comparison between frictional and cohesive models must be contextualized within their complexity and intended applications. The Norsand model, with its intricate structure and numerous parameters, offers a sophisticated approach. However, simpler models, such as the [19], might achieve comparable results in some scenarios.

## Conclusion

Gold mine tailings primarily consist of granular frictional materials, such as silt and sand, whose dilatancy behavior surpasses the limitations of simple associated plasticity assumptions,

such as those in Cam-clay theory. In this study, we adopt the framework developed in the Modified Glasgow Coupled Model (GCM) to extend constitutive models originally formulated for dry and saturated soils to unsaturated conditions. This framework is applied to the Norsand model, a widely used model for sands and silts, by introducing a yield surface extension in a third dimension dedicated to hydraulic state. Additionally, coupling terms are incorporated into the hardening laws governing both mechanical and hydraulic yield surfaces.

The diverse particle size distribution characteristic of hard rock tailings results in a broad soil-water characteristic curve (SWCC), which can exhibit significant hysteresis during drying and wetting cycles. To account for this, the GCM formulation is enhanced to better represent the evolution of saturation with suction.

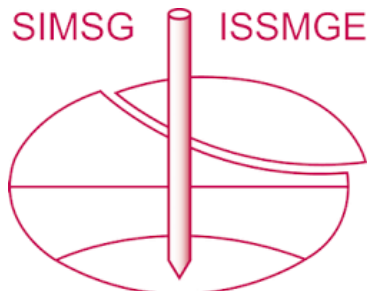
The extended model is calibrated using results from simple shear tests conducted on gold mine tailings. These tailings were desiccated to varying water content levels, re-saturated to simulate layered deposition, and then sheared under undrained conditions. The calibration process demonstrates that the model effectively captures the dependency of the shearing response on the initial wetting and drying cycles with satisfactory accuracy. This approach can be applied to other constitutive models to extend their applicability to partially saturated geomaterials.

## References

- [1] Shunchao Qi, Paul Simms, Farzad Daliri, and Sai Vanapalli. Coupling elasto-plastic behaviour of unsaturated soils with piecewise linear large-strain consolidation. *Géotechnique*, 70(6):518–537, 2020.
- [2] Paul Simms. 2013 colloquium of the canadian geotechnical society: Geotechnical and geoenvironmental behaviour of high-density tailings. *Canadian Geotechnical Journal*, 54(4):455–468, 2017.
- [3] Farzad Daliri, Hyunseung Kim, Paul Simms, and Siva Sivathayalan. Impact of desiccation on monotonic and cyclic shear strength of thickened gold tailings. *Journal of Geotechnical and Geoenvironmental Engineering*, 140(9):04014048, 2014.
- [4] Farzad Daliri, Paul Simms, and Siva Sivathayalan. Shear and dewatering behaviour of densified gold tailings in a laboratory simulation of multi-layer deposition. *Canadian Geotechnical Journal*, 53(8):1246–1257, 2016.
- [5] Delwyn G Fredlund and Hendry Rahardjo. *Soil mechanics for unsaturated soils*. John Wiley & Sons, 1993.
- [6] Ning Lu and William J. Likos. *Unsaturated Soil Mechanics*. J. Wiley, 2004.
- [7] Alan W Bishop. The principle of effective stress. *Teknisk ukeblad*, 39:859–863, 1959.
- [8] Jerome Duriez, Richard Wan, Mehdi Pouragha, and Félix Darve. Revisiting the existence of an effective stress for wet granular soils with micromechanics. *International Journal for Numerical and Analytical Methods in Geomechanics*, 42(8):959–978, 2018.

- [9] Eduardo E Alonso, Antonio Gens, and Alejandro Josa. A constitutive model for partially saturated soils. *Géotechnique*, 40(3):405–430, 1990.
- [10] Martí Lloret-Cabot, Marcelo Sánchez, and Simon J Wheeler. Formulation of a three-dimensional constitutive model for unsaturated soils incorporating mechanical–water retention couplings. *International Journal for Numerical and Analytical Methods in Geomechanics*, 37(17):3008–3035, 2013.
- [11] K.H Roscoe and JB Burland. On the generalized stress-strain behaviour of wet clay. In J. Heyman and F. A. Lekie, editors, *Engineering Plasticity*, pages 535–609. Cambridge University Press, London, England, 1968.
- [12] MG Jefferies. Nor-sand: a simle critical state model for sand. *Géotechnique*, 43(1):91–103, 1993.
- [13] Mina Mofrad, Mehdi Pouragha, and Paul Simms. Constitutive modelling of unsaturated gold tailings subjected to drying and wetting cycles. *International Journal for Numerical and Analytical Methods in Geomechanics*, 2023.
- [14] K Terzaghi. Theoretical soil mechanics john wiley and sons inc. *New York*, 314, 1943.
- [15] Mike Jefferies and Ken Been. *Soil liquefaction: a critical state approach*. CRC press, 2015.
- [16] Dawn Shuttle and Michael Jefferies. Norsand: description, calibration, validation and applications. In *Geo-Frontiers Conference 2005: Soil Constitutive Models: Evaluation, Selection, and Calibration*, pages 1–31, 2010.
- [17] GT Housby. The work input to an unsaturated granular material. *Géotechnique*, 47(1):193–196, 1997.
- [18] M Th Van Genuchten. A closed-form equation for predicting the hydraulic conductivity of unsaturated soils. *Soil science society of America journal*, 44(5):892–898, 1980.
- [19] RG Wan and PJ Guo. A simple constitutive model for granular soils: modified stress-dilatancy approach. *Computers and Geotechnics*, 22(2):109–133, 1998.

# INTERNATIONAL SOCIETY FOR SOIL MECHANICS AND GEOTECHNICAL ENGINEERING



*This paper was downloaded from the Online Library of the International Society for Soil Mechanics and Geotechnical Engineering (ISSMGE). The library is available here:*

<https://www.issmge.org/publications/online-library>

*This is an open-access database that archives thousands of papers published under the Auspices of the ISSMGE and maintained by the Innovation and Development Committee of ISSMGE.*

*The paper was published in the proceedings of the 4th Pan-American Conference on Unsaturated Soils (PanAm UNSAT 2025) and was edited by Mehdi Pouragh, Sai Vanapalli and Paul Simms. The conference was held from June 22nd to June 25th 2025 in Ottawa, Canada.*